Impermeable Robust Hydrogels via Hybrid Lamination

German A. Parada, Hyunwoo Yuk, Xinyue Liu, Alex J. Hsieh, and Xuanhe Zhao*

Hydrogels have been proposed for sensing, drug delivery, and soft robotics applications, yet most of these materials suffer from low mechanical robustness and high permeability to small molecules, limiting their widespread use. This study reports a general strategy and versatile method to fabricate robust, highly stretchable, and impermeable hydrogel laminates via hybrid lamination of an elastomer layer bonded between hydrogel layers. By controlling the layers' composition and thickness, it is possible to tune the stiffness of the impermeable hydrogels without sacrificing the stretchability. These hydrogel laminates exhibit ultralow surface coefficients of friction and, unlike common single-material hydrogels, do not allow diffusion of various molecules across the structure due to the presence of the elastomer layer. This feature is then used to release different model drugs and, in a subsequent experiment, to sense different pH conditions on the two sides of the hydrogel laminate. A potential healthcare application is shown using the presented method to coat medical devices (catheter, tubing, and condom) with hydrogel, to allow for drug release and sensing of environmental conditions for gastrointestinal or urinary tract.

Hydrogels, water-containing polymer networks, have been widely used in biomedical applications such as drug delivery, tissue engineering, tissue bulking agents, and contact lenses owing to their similar physiological and mechanical properties as natural tissues.[1–7] More recently, hydrogels have been explored intensively as material candidates for new applications such as medical tubing and catheters,[8–10] control elements in fluidic devices,[11–14] antifouling coatings,[15–19] and soft electronics and machines.[20–26] However, hydrogels' promise and potential in these new applications have been significantly hampered by their low mechanical robustness and permeability

to various molecules.[20,27–29] For example, the strength and fracture toughness of common hydrogels are usually much lower than the corresponding elastomers (e.g., silicone rubbers and latex) used for the abovementioned applications;[25–27] and water-soluble molecules and viruses may diffuse through hydrogels but not elastomers.[28–35] Despite recent success in developing hydrogels with extraordinary mechanical properties, the design of impermeable robust hydrogels has remained a challenge in the field.

Here, we report a general strategy and a simple method to design and fabricate hydrogel laminates that are highly stretchable, robust and impermeable to various types of compounds ranging from small-molecule chemicals to biomolecules and nanoparticles, but that still retain the high water content and slippery surface properties of hydrogels. The design strategy for the impermeable robust hydrogel laminates is schematically illustrated in **Figure 1**A. A layer of an impermeable elastomer is sandwiched between two layers of a stretchable and tough hydrogel that consists of a physically crosslinked dissipative polymer network and a covalently crosslinked stretchy polymer network. The stretchy polymer network in the hydrogel is covalently grafted to the elastomer chains to achieve robust bonding between hydrogel and elastomer layers, a method previously developed by our group.[25,36,37] The candidates for the elastomer layer include silicone rubbers such as polydimethyl siloxane (PDMS, Dow Corning) and Ecoflex (Smooth-On), latex, polyurethanes, and other natural or synthetic rubbers. For the tough hydrogel layers, alginate (ALG), chitosan (CHI), and hyaluronan are candidates for the physically crosslinked networks whereas polyacrylamide (PAAm), polyethylene glycol (PEG), and polyvinyl alcohol are candidates for the covalently-crosslinked stretchy networks. Benzophenone is used to activate the surfaces of the elastomer layers to enable covalent grafting of the stretchy networks of the hydrogels onto the elastomer chains,[25] illustrated in the right inset of Figure 1A.

As shown in Figure 1D, the resultant hydrogel–elastomer–hydrogel laminate incorporating a transparent elastomer layer (e.g., PDMS) looks almost identical to a sheet of hydrogel. Nevertheless, the laminates possess a set of properties and capabilities unachievable in existing hydrogels: (a) the laminates have high water content, slippery surfaces, and can be functionalized with biomolecules in the same fashion as common hydrogels.[38–40] (b) The laminates are robust, highly stretchable, and impermeable to molecules of various types and sizes across the
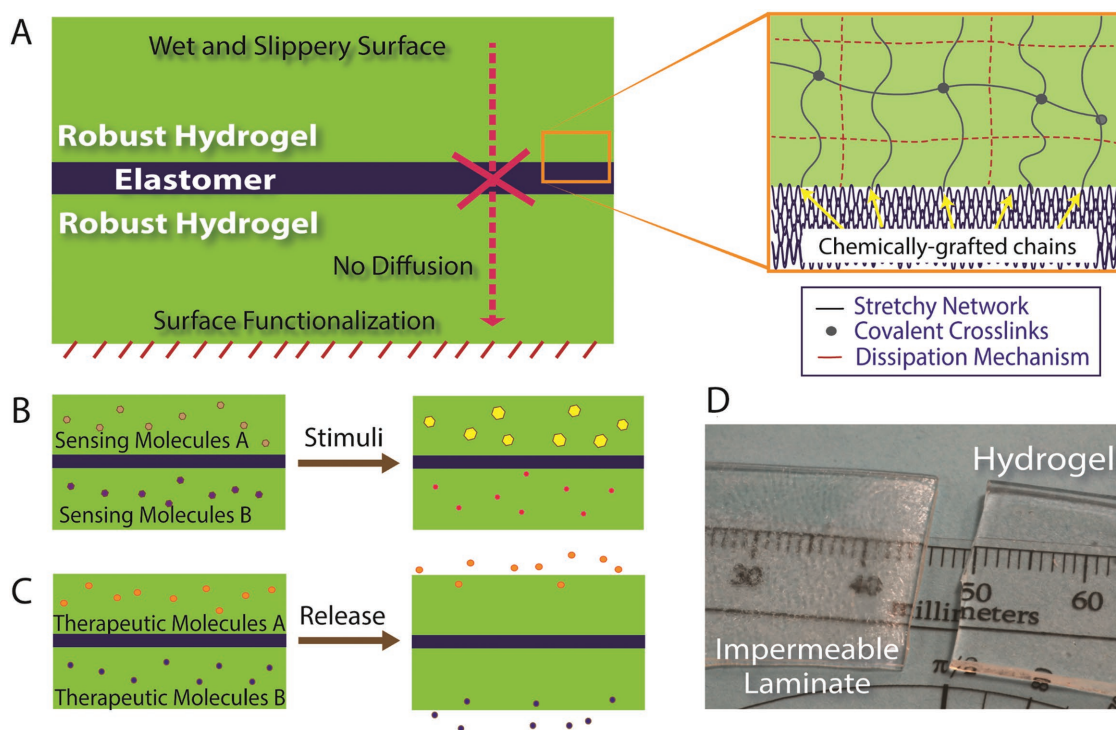
G. A. Parada, H. Yuk, X. Liu, Prof. X. Zhao
Soft Active Materials Laboratory
Department of Mechanical Engineering
Massachusetts Institute of Technology
Cambridge, MA 02139, USA
E-mail: zhaox@mit.edu
G. A. Parada
Department of Chemical Engineering
Massachusetts Institute of Technology
Cambridge, MA 02139, USA
Dr. A. J. Hsieh
U.S. Army Research Laboratory
RDRL-WMM-G
Aberdeen Proving Ground
MD 21005-5069, USA

The ORCID identification number(s) for the author(s) of this article can be found under https://doi.org/10.1002/adhm.201700520.

**ADVANCED
SCIENCE NEWS**
www.advancedsciencenews.com

**ADVANCED
HEALTHCARE
MATERIALS**
www.advhealthmat.de

Figure 1. Schematic and image of the impermeable hydrogel laminate. A) Structure of impermeable hydrogel laminates, major features and detailed hydrogel–elastomer interface network structure. B) Sensing capabilities for different environments of the impermeable hydrogel laminates. C) Release capabilities to different environments of the impermeable hydrogel laminates. D) Image of impermeable hydrogel laminate and hydrogel sheet showing that the laminates can achieve similar transparency as the pure hydrogel materials.
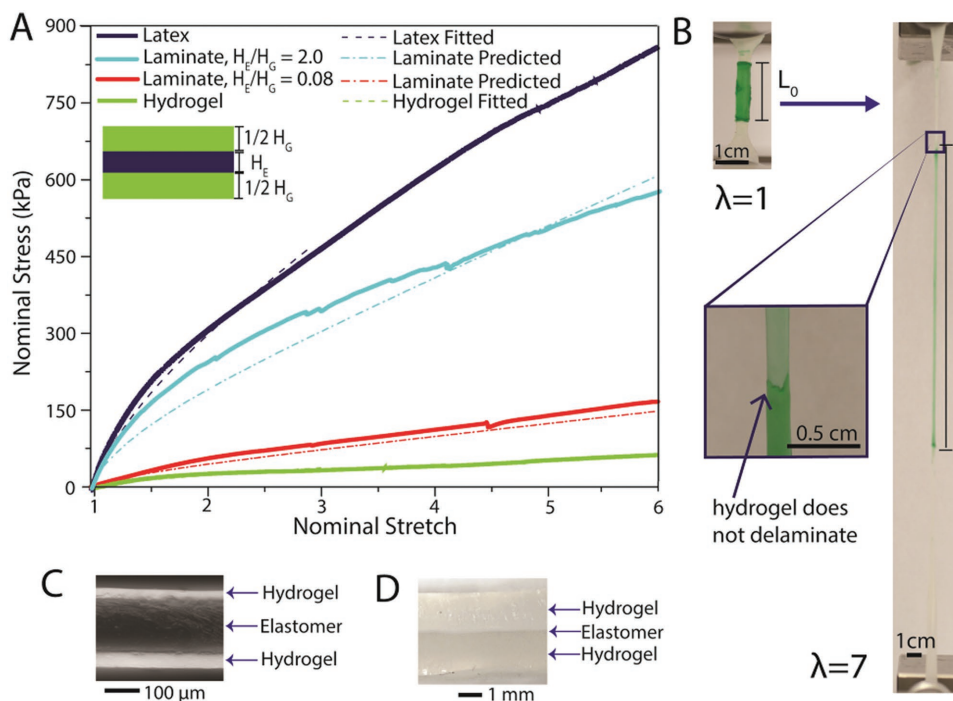
structure, similar to bulk elastomer sheets.[31,33] (c) The modulus of the laminate (along in-plane directions) can be tuned by varying the types of elastomer, type and composition of the hydrogel layers, and the thicknesses of the different layers. (d) Different sensing or stimuli-responsive molecules can be incorporated in different hydrogel layers of the laminate, as illustrated in Figure 1B, to monitor environmental conditions on both sides of the laminate (pH, temperature, and biomolecule concentration).[7,12,13,24,41–50] (e) Different types of drugs and functional molecules can also be incorporated into different hydrogel sheets of a laminate and released independently from both sides of the laminate,[7,46,49–52] as shown in Figure 1C.

The protocol for fabrication of the impermeable hydrogel laminates is described in full detail in the "Experimental Section" and outlined in Figure S1 of the Supporting Information. Briefly, a pristine elastomer sheet is immersed in a benzophenone solution in ethanol, rinsed with isopropanol and dried with compressed nitrogen. Hydrogel precursor solution, containing both stretchy and dissipative components along with sensing, stimuli-responsive or releasable molecules, is then placed on the activated elastomer surface, covered with a glass plate and cured in a UV oven. Upon exposure to UV light (λ = 365 nm), the adsorbed benzophenone molecules on the elastomer sheet act as free radical sources and grafting agents to the elastomers.[25] The thickness of the hydrogel layer is controlled by using spacers of different thicknesses. After curing this first hydrogel layer, the assembly is then flipped and the exposed elastomer surface is treated with benzophenone. Additional hydrogel precursor

solution is placed on the treated surface, covered, and cured again. The result is a hydrogel–elastomer–hydrogel structure with robust hydrogel layers well bonded to the elastomer sheet in the middle.

To characterize the in-plane mechanical properties of the laminate and individual components, uniaxial tensile tests are carried out with a mechanical testing machine at a strain rate of 1.0 min⁻¹. The chosen materials for the laminates are latex (McMaster Carr) elastomer and PAAm–ALG tough hydrogel (see the "Experimental Section" for full details). The samples are analyzed as prepared or after soaking in 1X phosphate buffer saline (PBS; Sigma-Aldrich) for 24 h. The solid dark blue and green curves on **Figure 2**A show the nominal stress versus stretch curves of as-prepared single-material latex and PAAm–ALG hydrogel samples, where the nominal stress is the applied force over un-deformed cross-sectional area of the sample, and the stretch is the deformed length of the sample over its un-deformed length. The latex underwent the same treatment as when fabricating the laminate but without addition of the hydrogel precursor. Both the latex and hydrogel samples can be highly stretched without failure, but their tensile properties are dramatically different. The shear modulus of latex is μ_E = 166.0 kPa and that of hydrogel is μ_H = 12.8 kPa, by fitting their stress–stretch curves to a neo-Hookean model.

For undeformed laminates, the thicknesses of the elastomer layer and the combined hydrogels layers are denoted as H_E and H_G, respectively (Figure 2A). Using the rule of mixture for composite materials, the shear modulus of the laminates can be calculated via

ADVANCED
SCIENCE NEWS

www.advancedsciencenews.com

ADVANCED
HEALTHCARE
MATERIALS

www.advhealthmat.de

Figure 2. Tensile properties of hydrogel and impermeable hydrogel laminates. A) Nominal stress versus stretch curves of elastomer, hydrogel, and laminates of varying elastomer-to-hydrogel thickness. Fit curves were obtained using the neo-Hookean model. B) Robust hydrogel–elastomer interface prevents delamination of impermeable hydrogel laminate (hydrogel dyed green for visualization) upon stretching up to seven times. C) Microscope image (hydrogel layers stained with fluorescent dye for visualization) of nonpermeable hydrogel laminate with $H_E/H_G = 2.0$. D) Image of nonpermeable hydrogel laminate with $H_E/H_G = 0.08$.

$$\mu = \frac{H_E}{H_E + H_G}\mu_E + \frac{H_G}{H_E + H_G}\mu_G \qquad (1)$$

Therefore, by varying the thickness ratio of elastomer and hydrogel layers in the laminate (i.e., H_E/H_G), the rigidity of the laminate can be tuned significantly. When the elastomer/hydrogel thickness ratio is small (e.g., $H_E/H_G = 0.08$, cross sectional image shown in Figure 2D), the stress versus stretch curve resembles that of a hydrogel sample, as shown by the red solid curve of Figure 2A. The broken red curve shows the predicted stress versus stretch curve from a neo-Hookean model using the shear modulus calculated using Equation (1). Conversely, if elastomer/hydrogel thickness ratio is large (e.g., $H_E/H_G = 2.0$, cross-sectional image shown in Figure 2C), the stress versus stretch curve is similar to that of the elastomer, as shown by the light blue curve in Figure 2A. Again, a neo-Hookean model is used to predict the broken light blue curve. To expand the modulus range of the hydrogel laminates, it is possible to use stiffer elastomers such as PDMS or gutta-percha rubbers, or more compliant hydrogels (featuring lower density of crosslinks). Furthermore, these laminates feature very robust bonding between the elastomer and hydrogel layers. As demonstrated in Figure 2B, no delamination is observed when stretching a sample of the laminate up to seven times of its original length.

In addition to having tunable tensile properties, the laminates are expected to have low coefficients of friction (COFs) due to the presence of slippery, high-water-content hydrogel on the surfaces of the laminate. Tribology measurements, following the methodology introduced by Chang et al.,[53] are carried out using an AR-G2 rotational rheometer in normal force control mode with parallel plate geometry. The COF is calculated from the measured torque and normal forces (see the "Experimental Section" for equations) and summarized in **Table 1**.

Utilizing the rheometer steel fixture as the top plate, the COF of the samples of hydrogel, wet latex, and hydrogel laminate (with latex as the elastomer layer and PAAm–CHI as the hydrogel layer, $H_E/H_G = 0.2$) against steel is measured at three different shear rates. While the COF of all samples increases with increasing shear rate, the COFs of the hydrogel and hydrogel laminate are identical (within experimental error) and consistently 3–5 times lower than the COF of wet latex (values provided in Table 1). Latex is then attached to the rheometer fixture and the COF of latex against samples of hydrogel laminate, and wet latex is measured. The same trend is observed as the COFs are 2–4 times lower across all tested shear rates in the hydrogel laminate than in the wet latex. Furthermore, the measured COF between two hydrogel laminates is even lower than the COFs of steel on hydrogel laminates and latex on hydrogel laminates across different shear rates. This measured COF (between two hydrogel laminates) is in agreement with the reported COF values between swollen hydrogels.[50,51] These results, which are expected to be independent of H_E/H_G, prove that the hydrogel laminates possess slippery surfaces similar to the corresponding hydrogels.

Table 1. Coefficient of friction (COF) for different surfaces as a function of shear rate. The COF of hydrogel conditions is lower than the wet latex conditions across all rates, with the hydrogel-on-hydrogel condition having the lowest COF measured.

| Surface Pair Condition	0.1 [s^{-1}]	0.5 [s^{-1}]	1.0 [s^{-1}]
Steel on wet latex	0.269 ± 0.049	0.363 ± 0.144	0.535 ± 0.089
Steel on hydrogel laminate	0.078 ± 0.008	0.096 ± 0.014	0.109 ± 0.013
Steel on hydrogel	0.082 ± 0.018	0.106 ± 0.016	0.169 ± 0.023
Latex on wet latex	0.216 ± 0.017	0.291 ± 0.081	0.545 ± 0.165
Latex on hydrogel laminate	0.082 ± 0.016	0.114 ± 0.020	0.145 ± 0.024
Hydrogel laminate on hydrogel laminate	0.022 ± 0.004	0.024 ± 0.001	0.023 ± 0.002

Next, we demonstrate the impermeability of hydrogel laminates through a set of diffusion, release and stimuli-response tests. To examine the diffusion properties of the hydrogel laminates, a two-chamber diffusion device, shown in **Figure 3**A, is employed.[28,54] Samples of hydrogel (PAAm–ALG), elastomer (latex), or the corresponding hydrogel laminate (PAAm–ALG and latex, $H_E/H_G = 0.05$) are placed between the two chambers containing a 5.0×10^{-4} M Rhodamine B (Sigma-Aldrich) solution and deionized water (DI water, Millipore). The concentration of rhodamine B diffusing to the water chamber is monitored

by measuring the absorbance at 550 nm on a spectrophotometer and converting this result to concentration using a calibration curve for known rhodamine B concentrations.

For the hydrogel sample, rhodamine B readily diffuses to the water chamber (Figure 3B, green data). This process can be described by a pseudosteady state, 1D diffusion model which predicts a linear relationship between time and the concentration of rhodamine B in the water chamber[54] (full derivation is in the "Experimental Section"). The diffusion coefficient, calculated from the slope of the fit line (dashed green curve), is $1.80 \cdot 10^{-7}$ cm^2 s^{-1} and is in agreement with previously-reported values.[20] For both elastomer and hydrogel laminate samples, there is no measurable diffusion of rhodamine to the water chamber over a 2 h period (Figure 3B, blue and red data), which demonstrates the impermeability of the laminate. Cross-sectional images of the hydrogel laminate and individual hydrogel samples after the diffusion test (Figure 3D and Figure 3E, respectively) provide a visual confirmation of this result. The diffusion of dye occurs readily across the hydrogel but is halted at the elastomer layer in the middle of the laminate.
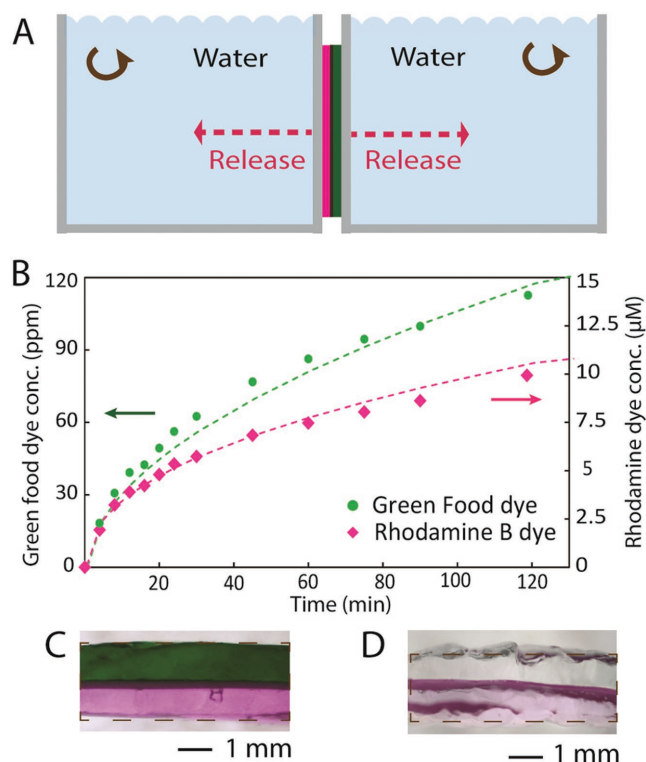
Taking advantage of the impermeability of hydrogel laminate, we then test the possibility of releasing different molecules from the two sides of the hydrogel sheets in the laminate. Green food dye (Fast Green FCF, Sigma-Aldrich) and rhodamine B are used as model drugs and are loaded to the two hydrogel sheets in the laminate sequentially. As shown in **Figure 4**A, the laminate is placed in the diffusion apparatus initially containing DI water in both chambers. The concentrations of green food dye and rhodamine B in the solutions of both chambers are measured over time using absorbance measurements.[54] The results show typical power law release profiles for both drugs over the course of the experiment (Figure 4B), indicating Fickian release from the hydrogel layers in the laminate (exponent ≈ 0.5). The cross-sectional pictures of the laminate before and after the experiment (Figure 4C and Figure 4D, respectively) provide a visual demonstration of the dye release. Since the dyes used have absorbance maximums at different wavelengths (550 and 630 nm), it is possible to detect dye leakage through the impermeable hydrogel laminate by monitoring the absorbance signals at the two wavelengths in both chambers. No green food dye can be detected in the rhodamine chamber and vice versa, further validating the impermeability of the hydrogel laminates, and the possibility of spatially controlled release from the two sides of the hydrogel laminate.

In addition to releasing molecules of interest to separate environments, the impermeable hydrogel laminates also enable
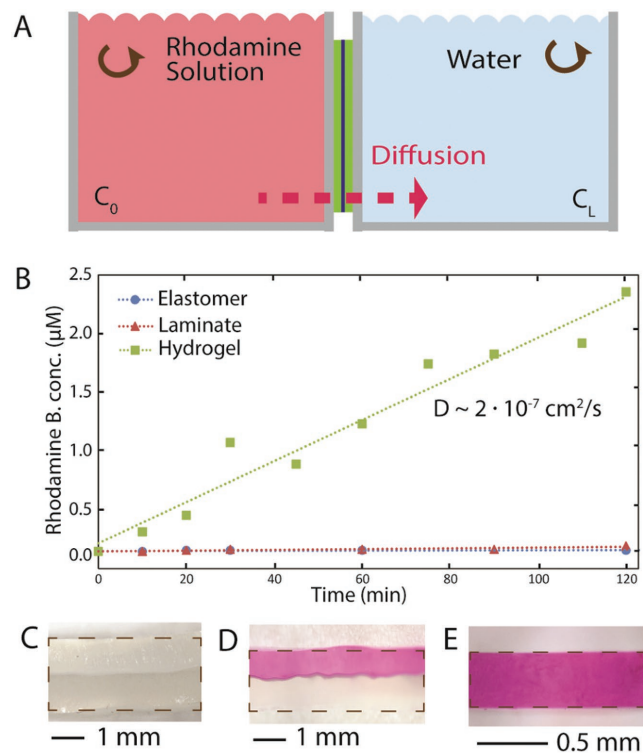
Figure 3. Diffusion characteristics of impermeable hydrogel laminates. A) Two-chamber experimental setup used to study diffusion characteristics. B) Diffusion curves of rhodamine B dye across elastomer, hydrogel slab, and impermeable hydrogel laminate samples, showing steady diffusion across the hydrogel slab and no diffusion on the elastomer and hydrogel laminate cases. C) Image of impermeable hydrogel laminate before diffusion experiment. D) Image of impermeable hydrogel laminate after diffusion experiment showing no dye diffusion past the elastomer layer. E) Image of pure hydrogel sheet after the diffusion experiment showing diffusion of the dye across the sample.

ADVANCED
SCIENCE NEWS
www.advancedsciencenews.com

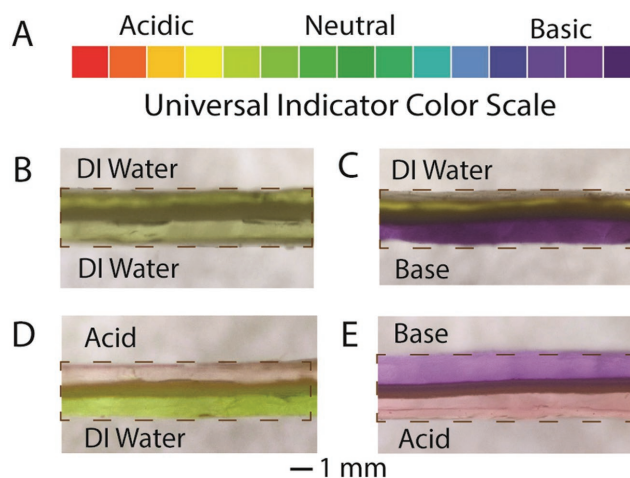**ADVANCED**
HEALTHCARE
MATERIALS
www.advhealthmat.de

Figure 4. Release characteristics of the hydrogel laminates to different environments. A) Two-chamber experimental setup to study drug release from impermeable hydrogel laminates to different environments. B) Release profiles of rhodamine B and green food dye to the separate chambers with Fickian diffusion power law fits. C) Loaded impermeable hydrogel laminate before the release experiment. D) Impermeable hydrogel laminate after the release experiment.


Figure 5. Sensing capabilities of impermeable hydrogel laminates. A) Color range as a function of pH of universal indicator solution used for sensing on both sides of the impermeable laminates. B–E) Sensing of different pH conditions on different sides of the impermeable hydrogel laminates.

sensing of different types of stimulus, or different conditions of the same stimulus on the two sides. To demonstrate this capability, we add universal indicator solution (Sigma-Aldrich) to the hydrogel layers as a visual pH indicator. Using the diffusion apparatus, the laminates are contacted for 3 min with solutions of different pH on the two sides and cross-sectional images were obtained. The resulting cross-sectional images can be seen in **Figure 5**B–E; there are clear visual differences on the hydrogel layers depending on the pH of the contacting solutions. The nonpermeable nature of the overall structures combined with the fast diffusion of small molecules within the hydrogel layers allows for fast sensing of different pH environments on the two sides of the nonpermeable hydrogel sheet. This capability, in combination with previously developed responsive hydrogel materials, can be utilized to sense biologically relevant parameters such as glucose, pH, ion concentration, or protein levels[7,41–44,47,50] in separate environments.

The unique capabilities of the hydrogel laminates to spatially control environmental sensing and drug release may be advantageous for healthcare applications in which these properties play a major role, such as wound and dermal care, and specific gastrointestinal and urinary tract treatments. For instance, hydrogel-coated catheters could be used to deliver anti-inflammatory drugs to the urethra while monitoring biomolecules present in the urine. The presence of hydrogel surfaces would,

in addition, decrease the irritation and discomfort caused by friction.[8–10] To demonstrate this concept, we coat the outer surface of several elastomeric medical devices using a modified hydrogel laminate protocol (described in the "Experimental Section" and Figure S2 in the Supporting Information). The images of silicone tubing (VWR International), a Foley catheter (Bard Medical), and a condom (Trojan) coated with a thin and uniform hydrogel layer are found in **Figure 6**. The hydrogel coating is robust and strongly bonded to the tubing (Figure 6A), and it does not delaminate upon folding the tubing in a knot or sharp bend (Figure 6B,C). The coated condom (Figure 6D) and catheter (Figure 6G) can be inflated without delamination of the hydrogel coating, as shown in Figure 6E–H. Since the hydrogel precursor is dip-coated to the devices, the resulting layer is very thin as shown in the cross-sectional images in Figure 6I–K.

These results demonstrate that the strategy introduced in this work can be used to create medical devices based on hydrogel–elastomer laminates. The high robustness and stretchability of the hydrogel–elastomer laminates can allow for proper functioning of the devices under stresses and deformations. The tough hydrogel coatings used in this study are biocompatible[28,36] and can prevent bacterial adhesion, as shown in Figure S3 in the Supporting Information. While the lubricious and highly hydrated surfaces are expected to improve the protein adsorption, anticlotting and foreign-body reaction of the devices as compared to the uncoated options, further work is needed to characterize these responses. Moreover, the coating protocol can be adjusted to include drugs in the hydrogel coating or to introduce hydrogel components with known biological responses such as PEG, hyaluronic acid, and zwitterionic groups.[55]

In summary, we present a strategy to combine the permeable, compliant, tunable, and slippery nature of tough hydrogels with the nonpermeable and relatively rigid properties of elastomers via hydrogel-laminate structures. Robust bonding of hydrogels and elastomer allows for the assembly of such structures, which can be stretched up to seven times without
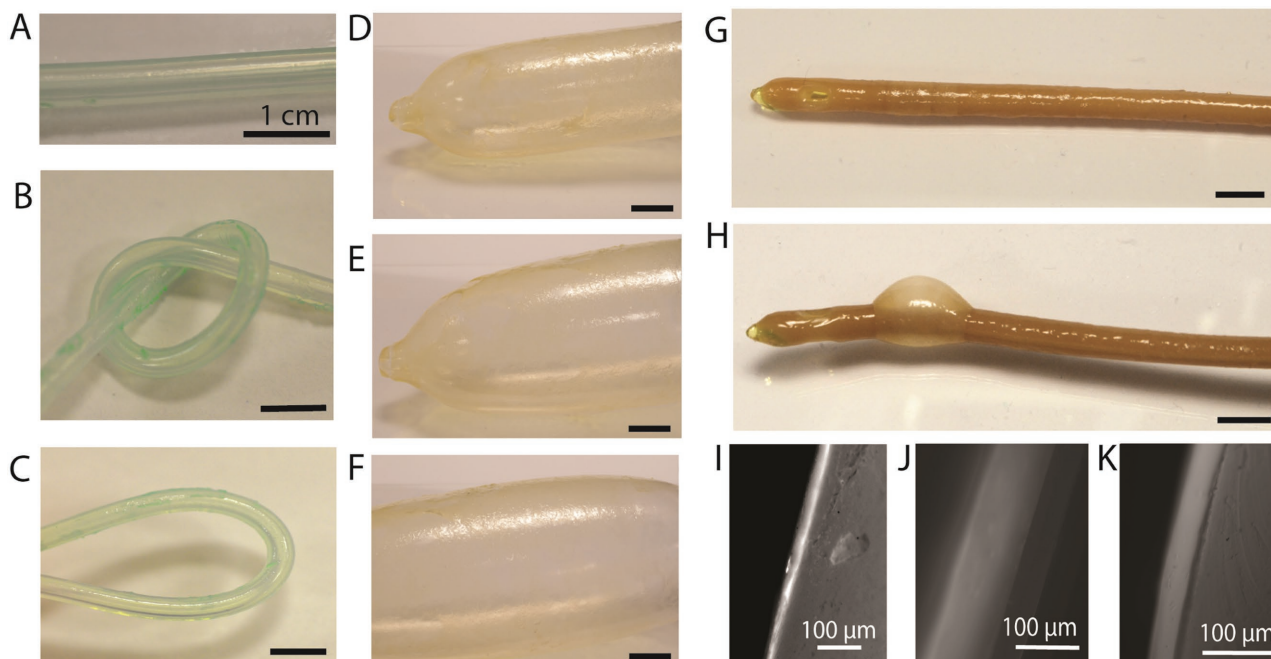
Figure 6. Coating of medical devices using the impermeable hydrogel laminate strategy. A) Hydrogel-coated silicone tubing stained by immersion in green food dye solution. B) The hydrogel layer remains on tubing after tying into a knot. C) The hydrogel layer remains on tubing after bending. D) Hydrogel-coated latex condom. E,F) The hydrogel layer remains on the condom after inflation. G) Hydrogel-coated latex Foley catheter. H) The hydrogel remains on the catheter after inflation of the catheter balloon to its maximum size. I–K) Fluorescent microscopy cross-sectional image of the I) hydrogel-coated tubing, J) condom, and K) catheter. The hydrogel layer is stained by immersing in fluorescein solution and it appears white (high fluorescence intensity) to the left of the elastomeric device (gray). The scale bars are all 1 cm unless indicated otherwise.

delaminating. These hydrogel laminates can be tuned to match a wide range of mechanical properties from pure elastomer to pure hydrogel while maintaining a surface with a very low coefficient of friction. In addition, these hydrogel sheets are impermeable to small molecules across the laminate structure, feature that enabled controlled release of different drugs, and sensing of different stimuli on the two sides. We then use the strategy introduced here to coat several medical devices with a tough hydrogel coating that can be used for sensing and releasing while reducing the surface friction of these devices.

Experimental Section

Fabrication of Impermeable Hydrogels: All chemicals used in this work were purchased from Sigma-Aldrich and used as received, unless indicated otherwise. The impermeable hydrogel laminates were made by bonding two hydrogel layers containing either acrylamide–alginate (AAm–ALG) or acrylamide–chitosan (AAm–CHI) to a thin elastomer sheet.

The acrylamide–alginate hydrogel was made by mixing 1 mL of a previously degassed aqueous pre-gel solution (12 wt% acrylamide (Sigma-Aldrich A8887), 2 wt% sodium alginate (Sigma-Aldrich A2033)) with 60 µL of 0.2 wt% N,N'-methylenebisacrylamide (BIS; Sigma-Aldrich 146072), 10 µL of 0.2 M ammonium persulfate (APS; Sigma-Aldrich A3678), 20 µL of 1.0 M calcium sulfate (Sigma-Alginate C3771), and 1.0 µL of N,N,N',N'-tetramethylethylenediamine (TEMED; Sigma-Aldrich T9281).

The acrylamide–chitosan hydrogel was made by mixing 1 mL of a previously degassed aqueous pre-gel solution (18 wt% acrylamide, 2 wt% chitosan (Sigma-Aldrich 740500), 2 wt% acetic acid

(Sigma-Aldrich 27225)) with 60 µL of 0.2 wt% BIS, 15 µL of 0.2 M APS, 60 µL of 0.5 M sodium tripolyphosphate (Sigma-Alginate 238503), and 1.0 µL of TEMED.

The elastomer sheets were cut from a latex roll (McMaster Carr), rinsed with isopropanol (Sigma-Aldrich W292907), and dried with a stream of nitrogen gas. Then, a 10 wt% benzophenone (Sigma-Aldrich B9300) solution in ethanol (Sigma-Aldrich 459844) was placed on the top surface for 1 min, and the sheet was rinsed with isopropanol and dried. The hydrogel pre-gel solution was quickly placed on top of the latex sheet and covered with a chlorosilane-treated (GlassFree, National Diagnostics) glass plate. Then, the assembly was placed in a UV oven (365 nm UV; UVP CL-1000) for 1 h to cure. The assembly was removed from the oven and flipped. The exposed latex surface was rinsed with isopropanol and treated with 10% benzophenone solution in ethanol, and dried with nitrogen. More hydrogel pre-gel precursor was poured, covered with a glass plate, and cured for another hour. The laminate was removed from the glass plates, and imaged and tested as prepared or after immersion in 1× PBS for 24 h.

Hydrogel Coating of Medical Devices: Silicone medical tubing (VWR International) was cut into ≈10 cm segments, rinsed with isopropanol (Sigma-Aldrich W292907), and dried with a stream of nitrogen gas. Then, individual segments were oxygen-plasma-treated for 45 s (30 W at a pressure of 350 mTorr; Harrick Plasma PDC-001), submerged for 60 s in a 10 wt% benzophenone (Sigma-Aldrich B9300) solution in ethanol (Sigma-Aldrich 459844), rinsed with isopropanol, and dried. The tubing segments were then dip-coated in a modified acrylamide–chitosan hydrogel precursor solution (composition detailed below) and cured by UV exposure (365 nm UV; UVP CL-1000) for 1 h inside a custom-made with a glass cover filled with nitrogen. After curing, the coated tubing was rinsed in PBS for 1 h before imaging. The catheter (Bard Medical BARDIA Latex Foley Catheter, 16 Fr.) and condom (Trojan ENZ) were coated using the same protocol but leaving the devices intact.

The modified acrylamide–chitosan hydrogel was made by mixing 1 mL of a previously degassed aqueous pregel solution (18 wt% acrylamide, 2 wt% chitosan, and 2 wt% acetic acid) with 40 mg of glucose (Sigma-Aldrich G5767), 30 µL of 1.0 wt % glucose oxidase (Sigma-Aldrich G2133), 60 µL of 0.2 wt% BIS, 15 µL of 0.2 M APS, 60 µL of 0.5 M sodium tripolyphosphate, and 1.0 µL of TEMED.

Imaging of Coated Medical Devices: The coated devices were cut with a sharp razor blade and immersed in a 1×10^{-3} M fluorescein (fluorescein sodium salt, Sigma-Aldrich 46960) aqueous solution for 1 min. The images were obtained using the built-in camera of a Nikon Eclipse LV100ND fluorescent microscope.

Mechanical Testing: All uniaxial tensile tests were conducted in ambient air at room temperature. The tests took place in a few minutes, so the change of properties due to dehydration was not significant. Pure hydrogel, elastomer, and impermeable hydrogel laminate samples were cut (approximate size: 5 cm × 1 cm) and stretched using a universal mechanical testing machine (2 kN or 20 N load cells; Zwick/Roell Z2.5) by gripping directly to the fixtures. The grip-to-grip separation speed was set to 20 mm min^{-1} for all tests, resulting in a nominal strain rate of 1.0 min^{-1}. All tests were done in triplicate.

Coefficient of Friction Testing: All tests were conducted at room temperature using a controlled stress rheometer AR-G2 (TA Instruments, New Castles, DE, USA) in normal force control mode with 20 mm steel parallel plate fixtures. Hydrogel, elastomer, and impermeable hydrogel laminate (approximate size: 4 cm × 4 cm) samples were cut and placed in between the fixtures for testing. After placing the solvent trap, filling with water to minimize dehydration and zeroing the forces, a normal force of 0.4 N was applied to the sample. The sample was allowed to equilibrate for 10 min, then a set shear rate (0.1, 0.5, 1.0 s^{-1}) was established. After a 10 min equilibration interval, torque was measured over a 10 min interval. Following published methodology,[53] the friction force (F_R) was calculated using Equation (2), below, where T is the torque and R is the radius of the parallel plate fixture. The COF was obtained by dividing the time-averaged friction force over the time-averaged normal force (N), as shown in Equation (3). All tests were done in triplicate, and the standard deviation was reported

$$F_R = \frac{4T}{3R} \tag{2}$$

$$COF = \frac{\overline{F_R}}{\overline{N}} \tag{3}$$

Diffusion, Release, and Sensing Testing: A two-chamber diffusion device was made using cast acrylic plates (McMaster Carr), and small magnetic stir bars and stir plates (VWR International) were used for stirring. For the diffusion tests, a 3 cm × 3 cm hydrogel, elastomer, or impermeable hydrogel laminate sample was placed between the chambers and screwed tightly to prevent leakage from the chambers. A 5.0×10^{-4} M rhodamine B solution (Sigma-Aldrich R6626) was placed on one chamber while DI water was placed in the opposite chamber, and 1 mL aliquots were taken every 10 min and placed in a disposable cuvette. Absorbance was measured using a spectrophotometer (BioMate 3S, ThermoFischer Scientific) and converted to concentration using calibration curves of solutions with known concentrations. The setup for release experiments was identical except both chambers initially contained DI water with rhodamine B and green food dye (Fast green FCF, Sigma-Aldrich F7252) being released from the hydrogel. For rhodamine diffusion and release, a wavelength sweep was performed to determine the maximum absorbance, which occurred at 550 nm. The calibration curve was constructed by measuring absorbance of standard solutions in the $0–50 \times 10^{-6}$ M range. For green food dye release, the maximum absorbance occurred at 630 nm. The calibration curve was constructed by measuring absorbance of standard solutions in the 0–200 ppm range.

To calculate the diffusion coefficient of the PAAm–ALG hydrogel, a simple pseudosteady state was employed as the chamber volume was much larger than the hydrogel sample volume and the characteristic diffusion time scale across the hydrogel membrane[20] ($t_D = L^2/D \approx 3$ min) was smaller than the experiment time scale (≈ 120 min). Therefore, the transient contribution of the diffusion equation can be neglected. Moreover, due to the geometry of the system, the diffusion can be assumed to be unidimensional, so the full diffusion equation can be simplified to

$$D\frac{\partial^2 c}{\partial x^2} = \frac{\delta c}{\delta t} = 0 \tag{4}$$

The solution to this equation is the linear expression as shown below, where c_L and c_0 are the downstream and upstream concentrations, and L is the thickness of the sample. However, since c_0 is much higher than c_L throughout the experiment, the solution can be further simplified

$$c(x) = c_0 + \frac{c_L - c_0}{L}x \approx c_0\left(1 - \frac{x}{L}\right) \tag{5}$$

The flux of dye (J) was calculated from Fick's first law of diffusion ($J = -D$ (dc/dx)) and equated to the flux corresponding to the change in concentration of the downstream chamber ($J = c_L V_D/At$), where V_D is the chamber volume, A is the sample area normal to the diffusion direction, and t is the time. This yields Equation (6)

$$\frac{c_L V_D}{At} \approx KD\frac{c_0}{L} \tag{6}$$

In this expression, K is the dye partition coefficient. By taking the time derivative of this expression and rearranging, Equation (7) is obtained, which indicates that the slope of normalized concentration (c_L/c_0) versus time will be directly proportional to the diffusion coefficient[54]

$$\frac{d}{dt}\left(\frac{c_L}{c_0}\right) \approx \frac{KDA}{LV_D} \tag{7}$$

For the rhodamine B diffusion experiment, the measured value of $KD = 1.80 \times 10^{-7}$ cm^2 s^{-1}. Assuming $K \approx 1$, the value was in good agreement with previously published diffusion coefficient values.[20]

Bacterial Adhesion Testing: An engineered *Escherichi coli* strain expressing green fluorescent protein previously used by this group[27] was cultured in a 24-well plate above 8 mm round samples of latex, glass or swollen hydrogel laminate (PAAm–ALG and PAAm–CHI, as described previously). Streptomycin sulfate (Sigma-Aldrich S9137) was added to the two laminate formulations, at a final concentration of 0.1 wt%. After incubating at 37 °C for 24 h, the samples were removed, rinsed with PBS to remove free-floating bacteria, and imaged with a fluorescent microscope (Nikon Eclipse LV100ND).

Supporting Information

Supporting Information is available from the Wiley Online Library or from the author.

Acknowledgements

Conflict of Interest

The authors declare no conflict of interest.

Keywords

hydrogel devices, impermeable, laminate structures, lubricious surfaces, tough hydrogels

[1] J. L. Drury, D. J. Mooney, *Biomaterials* **2003**, *24*, 4337.

[2] O. Chaudhuri, L. Gu, D. Klumpers, M. Darnell, A. A. Bencherif, J. C. Weaver, N. Huebsch, H. P. Lee, E. Lippens, G. N. Duda, D. J. Mooney, *Nat. Mater.* **2016**, *15*, 326.

[3] M. P. Lutolf, J. A. Hubbell, *Nat. Biotechnol.* **2005**, *23*, 47.

[4] P. Gupta, K. Vermani, S. Garg, *Drug Discovery Today* **2002**, *7*, 569.

[5] T. R. Hoare, D. S. Kohane, *Polymer* **2008**, *49*, 1993.

[6] A. Miserez, J. C. Weaver, O. Chaudhuri, *J. Mater. Chem. B* **2015**, *3*, 13.

[7] Y. Qiu, K. Park, *Adv. Drug Delivery Rev.* **2012**, *64*, 49.

[8] R. A. Bologna, L. M. Tu, M. Polansky, H. D. Fraimow, D. A. Gordon, K. E. Whitmore, *Urology* **1999**, *54*, 982.

[9] P. Francois, P. Vaudaux, N. Nurdin, H. J. Mathieu, P. Descouts, D. P. Lew, *Biomaterials* **1996**, *17*, 667.

[10] K. K. Lai, S. A. Fontecchio, *Am. J. Infect. Control* **2002**, *30*, 221.

[11] S. E. Bakarich, R. Gorkin, M. I. H. Panhuis, G. M. Spinks, *Macromol. Rapid Commun.* **2015**, *36*, 1211.

[12] S. Naficy, G. M. Spinks, G. G. Wallace, *ACS Appl. Mater. Interfaces* **2014**, *6*, 4109.

[13] S. Naficy, G. M. Spinks, G. G. Wallace, in *Electroactive Polymer Actuators and Devices (EAPAD) 2014* (Ed: Y. Bar-Cohen), SPIE, San Diego, USA **2014**, p. 9056.

[14] N. A. Peppas, J. Z. Hilt, A. Khademhosseini, R. Langer, *Adv. Mater.* **2006**, *18*, 1345.

[15] S. Chen, C. Zhao, M. Zhang, Q. Chen, J. Ma, J. Zheng, *Langmuir* **2016**, *23*, 3315.

[16] T. Ekblad, G. Bergstroem, T. Ederth, S. L. Conlan, R. Mutton, A. S. Clare, S. Wang, Y. L. Liu, Q. Zhao, F. D'Souza, G. T. Donnelly, P. R. Willemsen, M. E. Pettitt, J. A. Callow, B. Liedberg, *Biomacromoles* **2008**, *9*, 2775.

[17] N. Ahmed, T. Murosaki, A. Kakugo, T. Kurokawa, J. P. Gong, Y. Nogata, *Soft Matter* **2011**, *7*, 7281.

[18] T. Murosaki, N. Ahmed, J. P. Gong, *Sci. Technol. Adv. Mater.* **2011**, *12*, 6.

[19] H. Chen, Q. Chen, R. Hu, H. Wang, B.-M. Z. Newby, Y. Chang, J. Zheng, *J. Mater. Chem. B* **2015**, *27*, 5426.

[20] S. Lin, H. Yuk, T. Zhang, G. A. Parada, H. Koo, C. Yu, X. Zhao, *Adv. Mater.* **2016**, *28*, 4497.

[21] L. Ionov, *Mater. Today* **2014**, *17*, 494.

[22] G. Stoychev, S. Turcaud, J. W. C. Dunlop, L. Ionov, *Adv. Funct. Mater.* **2012**, *23*, 2295.

[23] L. Ionov, *Adv. Funct. Mater.* **2013**, *23*, 4555.

[24] A. Tamayol, M. Akbari, Y. Zilberman, M. Comotto, E. Lesha, L. Serex, S. Bagherifard, Y. Chen, G. Q. Fu, S. K. Ameri, W. T. Ruan, E. L. Miller, M. Dokmeci, S. Sonkusale, A. Khademhosseini, *Adv. Healthcare Mater.* **2016**, *5*, 711.

[25] H. Yuk, T. Zhang, G. A. Parada, X. Liu, X. Zhao, *Nat. Commun.* **2016**, *7*, 12028.

[26] H. Yuk, S. Lin, C. Ma, M. Takkafoli, N. Fang, X. Zhao, *Nat. Commun.* **2017**, *8*, 14230.

[27] X. Liu, T.-C. Tang, E. Tham, H. Yuk, S. Lin, T. Lu, X. Zhao, *Proc. Natl. Acad. Sci. USA* **2017**, *114*, 2200.

[28] J. Y. Sun, X. Zhao, W. R. K. Illeperuma, O. Chaudhuri, K. H. Oh, D. J. Mooney, J. J. Vlassak, Z. G. Suo, *Nature* **2012**, *489*, 133.

[29] B. A. Westrin, A. Axelsson, G. Zacchi, *J. Controlled Release* **1994**, *30*, 189.

[30] S. H. Gehrke, J. P. Fisher, M. Palasis, M. E. Lund, *Ann. N. Y. Acad. Sci.* **1997**, *831*, 179.

[31] R. F. Carey, W. A. Herman, S. M. Retta, J. E. Rinaldi, B. A. Herman, T. W. Athey, *Sex. Transm. Dis.* **1992**, *19*, 230.

[32] M. B. Cleenewerck, *Eur. J. Dermatol.* **2010**, *20*, 434.

[33] C. P. Hamann, J. R. Nelson, *Am. J. Infect. Control* **1993**, *21*, 289.

[34] R. M. Schek, S. J. Hollister, P. H. Krebsbach, *Mol. Ther.* **2004**, *9*, 130.

[35] O. Lieleg, K. Ribbeck, *Trends Cell Biol.* **2011**, *21*, 543.

[36] H. Yuk, T. Zhang, S. T. Lin, G. A. Parada, X. H. Zhao, *Nat. Mater.* **2016**, *15*, 190.

[37] T. Zhang, H. Yuk, S. Lin, G. Parada, X. Zhao, *Acta Mech. Sin.*, **2017**, *33*, 543 .

[38] T. Chaudhuri, F. Rehfeldt, H. L. Sweeney, D. E. Discher, *Methods Mol. Biol.* **2010**, *621*, 185.

[39] V. Damljanovic, B. C. Lagerholm, K. Jacobson, *Biotechniques* **2005**, *39*, 847.

[40] S. R. Caliari, J. A. Burdick, *Nat. Methods* **2016**, *13*, 405.

[41] A. N. Wilson, A. Guiseppi-Elie, *Adv. Healthcare Mater.* **2013**, *2*, 520.

[42] Z. Y. Xiao, R. A. L. Wylie, E. R. L. Brisson, L. A. Connal, *J. Polym. Sci., Part A: Polym. Chem.* **2016**, *54*, 591.

[43] S. F. Liu, J. R. Niu, Z. Y. Gu, *J. Appl. Polym. Sci.* **2009**, *112*, 2656.

[44] H. Yao, C. Marcheselli, A. Afanasiev, I. Lahdesmaki, B. A. Parviz, in *2012 IEEE 25th Int. Conf. Micro Electro Mechanical Systems (MEMS)* (Eds: L. Buchaillot, H. Zappe), IEEE, Paris, France **2012**.

[45] X. Guo, C. F. Wang, Y. A. Fang, L. Chen, S. Chen, *J. Mater. Chem.* **2011**, *21*, 1124.

[46] P. D. Thornton, R. J. Mart, S. J. Webb, R. V. Ulijn, *Soft Matter* **2008**, *4*, 821.

[47] J. Z. Hilt, M. E. Byrne, N. A. Peppas, *Chem. Mater.* **2006**, *18*, 5869.

[48] H. Meng, J. Zheng, X. Wen, Z. Cai, J. Zhang, T. Chen, *Macromol. Rapid Commun.* **2015**, *36*, 533.

[49] P. D. Thornton, R. J. Mart, R. V. Ulijn, *Adv. Mater.* **2007**, *19*, 1252.

[50] R. V. Ulijn, N. Bibi, V. Jayawarna, P. D. Thornton, S. J. Todd, R. J. Mart, A. Smith, J. E. Gough, *Mater. Today* **2007**, *10*, 40.

[51] A. Vashist, Y. K. Gupta, S. Ahmad, *J. Mater. Chem. B* **2014**, *2*, 147.

[52] N. J. Bhattarai, J. Gunn, M. Q. Zhang, *Adv. Drug Delivery Rev.* **2010**, *62*, 83.

[53] D. P. Chang, J. E. Dolbow, S. Zauscher, *Langmuir* **2007**, *23*, 250.

[54] A. G. Bajpayee, C. R. Wong, M. G. Bawendi, E. H. Frank, A. J. Grodzinsky, *Biomaterials* **2014**, *35*, 538.

[55] S. Chhen, S. Jiang, *Adv. Mater.* **2008**, *20*, 335.